



## Article

# Hydroxyethyl Starch, a Synthetic Colloid Used to Restore Blood Volume, Attenuates Shear-Induced Distortion but Accelerates the Convection of Sodium Hyaluronic Acid

Tsuneo Tatara

Department of Anesthesiology, School of Medicine, Hyogo Medical University, 1-1 Mukogawa-cho, Nishinomiya 663-8501, Hyogo, Japan; ttatara@hyo-med.ac.jp

**Abstract:** Hyaluronic acid (HA) plays important roles in tissue hydration and the transport of fluid and solutes through the interstitium. Hydroxyethyl starch (HES) solution is a synthetic colloid solution used during surgery. As HES leaks into the interstitium under inflammatory conditions during surgery, the effects of HES on HA's structure and distribution are of clinical relevance. To examine these under fluid shear stress, dynamic shear moduli of 0.1% sodium hyaluronic acid (NaHA) solution with or without HES during shear stress loading were measured using a rotational rheometer for 8 h. The loss shear modulus of NaHA in 0.15 M NaCl solution decreased over time by 30% relative to that before shear stress loading. The presence of 1% and 2% HES reduced the decrease in loss shear modulus of NaHA solution to 20% and 4%, respectively. To investigate the convective transport of 0.1% fluorescein-labeled hyaluronic acid (FHA) by infusion of 0.15 M NaCl or HES solution, the absorbance of FHA in a UV flow cell was continuously measured. HES solution of 0.5% increased transported FHA quantities by 120% compared to 0.15 M NaCl solution. HES-induced attenuation of shear-induced distortion of HA and acceleration of convective transport of HA should be considered during surgery.



**Citation:** Tatara, T. Hydroxyethyl Starch, a Synthetic Colloid Used to Restore Blood Volume, Attenuates Shear-Induced Distortion but Accelerates the Convection of Sodium Hyaluronic Acid. *Polysaccharides* **2024**, *5*, 598–608. <https://doi.org/10.3390/polysaccharides5040038>

Academic Editor: Karin Stana Kleinschek

Received: 20 July 2024

Revised: 6 October 2024

Accepted: 8 October 2024

Published: 10 October 2024



**Copyright:** © 2024 by the author. Licensee MDPI, Basel, Switzerland. This article is an open access article distributed under the terms and conditions of the Creative Commons Attribution (CC BY) license (<https://creativecommons.org/licenses/by/4.0/>).

**Keywords:** hyaluronic acid; hydroxyethyl starch; interstitium; shear stress; convection; surgery

## 1. Introduction

The interstitium, a space between cells and blood vessels, is a soft matter consisting of a network of coarse fibrous proteins such as collagen immersed in a highly hydrated matrix of fine fibrous structures containing glycosaminoglycans and proteoglycans [1]. One of the glycosaminoglycans found in the interstitium is hyaluronic acid (HA) [2], a high-molecular-weight linear polysaccharide polymer consisting of repeating disaccharide units of  $\beta$ -D-glucuronic acid and *N*-acetyl- $\beta$ -D-glucosamine [3]. HA, which forms a fibrous network at semi-diluted concentrations (approximately 0.6 mg/mL) [4], is presumed to exist in a physically entangled state at physiological concentrations (1–10 mg/mL) [1,2]. As HA concentration increases, the hydrodynamic interactions between HA chains are more pronounced, resulting in a stiffer HA structure with increased viscoelasticity [3]. These HA structures are stabilized by intramolecular and intermolecular interactions via hydrogen bonds between adjacent sugar residues [3]. Therefore, HA in the interstitium absorbs water by osmotic swelling and thus forms a gel-like structure [5,6]. This inherent HA structure is important from a clinical perspective because the resulting low hydraulic conductivity prevents tissue dehydration around cells, withstands mechanical deformation of tissue, and impedes the spread of cells (e.g., bacteria) in the interstitium [7].

On the other hand, HA's distribution in the interstitium enters a dynamic state where the concentration and molecular weight of HA in the interstitium depend on the balance between the synthesis and degradation of HA, both of which are accelerated under inflammatory conditions [8,9]. Moreover, a part of HA in the interstitium is washed out into

lymph vessels by interstitial fluid flow [6]. Nevertheless, due to the extremely inhomogeneous fibrous structure of the interstitium consisting of collagen, proteoglycan, and HA, the flow rate of interstitial fluid largely varies within the interstitium. Consistent with this, the velocity of interstitial fluid flow is assumed to widely range from 0.1 to 2  $\mu\text{m/s}$  [10], with large increases observed in inflammatory tissue [10] and cancer tissue [11]. Thus, the convective transport of HA plays a key role in the distribution of HA in the interstitium.

Hydroxyethyl starch (HES) solution is a synthetic colloid solution modified from waxy maize starch largely composed of highly branched amylopectin. HES solution is widely used to correct blood volume in patients undergoing major surgery when a decrease in blood volume occurs due to hemorrhage and inflammation [12]. However, intravenously infused HES can leak into the interstitium as a result of increased capillary permeability caused by inflammation during surgery [13], causing possible adverse effects such as renal dysfunction [12]. Despite the clinical relevance of the effects of HES on HA's structure and distribution in the interstitium, studies investigating these effects from a biophysical viewpoint are limited. It is possible that HA conformation in the interstitium is changed by the local environment, including the presence of interacting species [3] such as HES.

HA and HES both have a polysaccharide structure. Previous studies report that the addition of sugar and short-chain HA increases the dynamic moduli of HA [14]. The polysaccharidal nature of these molecules may explain the structural changes in HA resulting from restricted osmotic swelling due to altered solvent–polymer interactions, or increased bond angle restriction and steric hindrance to internal rotations due to the new hydrogen bonds created [15]. In particular, hydrogen bonds between adjacent saccharides largely contribute to the intrinsic stiffness of HA under physiological pH and electrolyte concentrations [16]. Consistent with these, HES decreases the intrinsic viscosity of sodium hyaluronic acid (NaHA) [17] and thereby accelerates solute diffusion through NaHA solution [18]. However, as HA in the interstitium is subject to the aforementioned interstitial fluid flow, findings obtained in an equilibrium or steady-state condition may be insufficient to describe time-dependent effects of HES on HA structure and distribution in the interstitium. Accordingly, the present study aimed to investigate the effects of HES on the hydraulic conductivity of NaHA solution, dynamic viscoelastic properties of NaHA during shear stress loading, and convective transport of NaHA.

## 2. Materials and Methods

### 2.1. Materials

This study used a commercially available 6% (*w/v*) HES solution with an average weight  $M_W$  of 130,000 (waxy maize starch-based HES: molar substitution, 0.41;  $C_2/C_6$  ratio, 9:1; Voluven<sup>®</sup>, Fresenius Kabi, Bad Homburg, Germany) [12]. This HES solution was diluted with 0.15 M NaCl solution to desired concentrations. NaHA from *Streptococcus equi* ( $M_W$   $1.3 \times 10^6$ ) [17] and fluorescein-labeled HA (FHA: approximate  $M_W$   $0.64\text{--}1.0 \times 10^6$ ) were purchased from Sigma-Aldrich (St. Louis, MO, USA). All reactions were carried out using purified water from a Millipore Milli-Q purification system (Merck Millipore, Burlington, MA, USA). HES solution was filtered through a 0.45  $\mu\text{m}$  membrane prior to use.

### 2.2. Hydraulic Conductivity of NaHA Solution

NaHA was dissolved in 0.15 M NaCl solution to prepare 0.1%, 0.15%, 0.2%, 0.3%, 0.4%, and 0.5% (*w/w*) solutions and left for 24 h to solidify with gentle stirring (approximately 20 rpm) at room temperature. Hydraulic conductivity ( $\kappa$ ) of each NaHA solution was measured using an ultra-fast double-sided reusable sample dialyzer<sup>™</sup> (outer diameter, 2.5 cm; chamber volume, 500  $\mu\text{L}$ ; 7404-5001D, Harvard Apparatus, Holliston, MA, USA), as previously reported (Figure 1) [18]. In this system, 0.5 mL of NaHA solution was interposed between two pre-cut cellulose acetate dialysis membranes (molecular weight cut-off 300,000; 7403-CA300K, Harvard Apparatus, Holliston, MA, USA), and 0.15 M NaCl solution or 1% (*w/v*) HES solution in a 20 mL polypropylene syringe (Terumo, Tokyo, Japan) was infused into the dialysis chamber containing NaHA solution via a connecting

tube (pressure-resistant tube, 2.6 mm in outer diameter, 1.2 mm in inner diameter; Edwards LifeSciences, Irvine, CA, USA) using an automatic infusion pump (syringe type, FP-2200, MELQUEST, Toyama, Japan) at a constant rate ( $Q$ ) of 1–4  $\mu\text{L}/\text{min}$ . Dialysis membranes were attached to a stainless mesh (24.8 mm in diameter, 0.3 mm in thickness, 1 mm in pore size, 15 mm in mesh area diameter) to prevent membrane distortion due to increased hydrostatic pressure. The pressure tube (pressure-resistant tube described above) was connected to a manometric chamber fitted with an electronic pressure transducer (PGM-1KG, Kyowa, Tokyo, Japan). Hydrostatic pressure in the pressure tube was continuously recorded every 100 s using LabVIEW<sup>®</sup> (National Instruments, Austin, TX, USA), which was found to steeply increase with time and then reach a plateau over 1–70 h. Experiments were repeated at least in triplicate at room temperature.

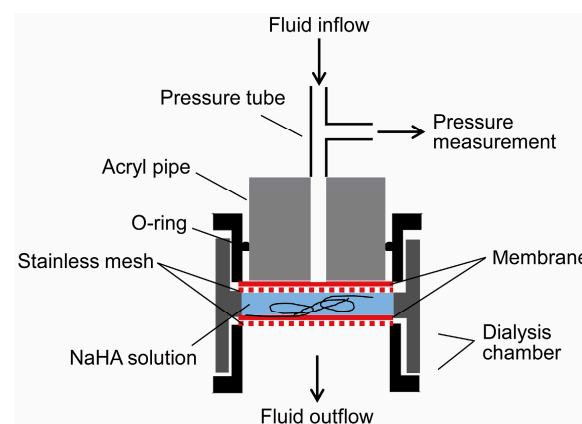


**Figure 1.** Experimental set-up for the measurement of hydraulic conductivity of sodium hyaluronic acid (NaHA) solution. Fluid (i.e., 0.15 M NaCl solution or 1% hydroxyethyl starch solution) was infused into the dialysis chamber containing 0.5 mL NaHA solution between semipermeable membranes at a constant rate, and hydrostatic pressure in the pressure tube was continuously recorded.

The value of  $\kappa$  ( $\text{cm}^4 \cdot \text{s}^{-1} \cdot \text{dyn}^{-1}$ ) was calculated according to Darcy's law by the linear fitting procedure using GraphPad Prism 5<sup>®</sup> software (GraphPad Software Inc., San Diego, CA, USA), as follows [1]:

$$\kappa = \frac{l}{A} \cdot \frac{1}{(\Delta P / \Delta Q)}, \quad (1)$$

where  $A$  is the membrane surface area available for fluid filtration ( $0.75^2 \times 3.14 = 1.77 \text{ cm}^2$ ),  $l$  is the thickness of NaHA solution in the dialysis chamber (0.28 cm, calculated as  $0.5/A$ ),  $\Delta P$  ( $\text{dyn}/\text{cm}^2$ ) is the difference in hydrostatic pressure in the pressure tube at plateau, and  $\Delta Q$  is the difference of  $Q$ .

Collective diffusion of particles is determined by the balance between the thermodynamic force that drives the spreading of solute particles and the frictional force that resists the spreading [19]. Accordingly,

$$D_{cc} = \kappa \cdot K + 43G, \quad (2)$$

where  $D_c(c)$  is the collective diffusion coefficient ( $\text{cm}^2/\text{s}$ ) of solute particles at a given concentration ( $c$ ,  $\text{g}/\text{cm}^3$ ),  $\kappa$  is the hydraulic conductivity in  $\text{cm}^4 \cdot \text{s}^{-1} \cdot \text{dyn}^{-1}$ ,  $K$  is the osmotic modulus in  $\text{dyn}/\text{cm}^2$  (which is equal to  $c(\delta\Pi/\delta c)$ , where  $\Pi$  is the osmotic pressure in  $\text{dyn}/\text{cm}^2$ ), and  $G$  is the shear modulus in  $\text{dyn}/\text{cm}^2$ . Since  $G$  of the NaHA solution was much smaller ( $<10 \text{ dyn}/\text{cm}^2$ ) than  $K$  ( $>100 \text{ dyn}/\text{cm}^2$ ) at all concentrations in this study, it was considered acceptable to neglect the  $G$  term in Equation (1) and describe  $D_c$  as follows:

$$D_{cc} = \kappa \cdot c \cdot \partial\Pi/\partial c, \quad (3)$$

As HES did not significantly affect  $\Pi$  of the NaHA solution (Figure S1 in Supplementary File),  $\Pi$  of the NaHA solution was given according to the literature, as follows [20]:

$$\Pi = 5.9 \times 10^4 \cdot c + 6.3 \times 10^7 \cdot c^2 \quad (4)$$

### 2.3. Dynamic Shear Moduli of NaHA Solutions during Shear Stress Loading

NaHA was dissolved in 0.15 M NaCl solution to prepare 0.1% (*w/w*) solution with or without 1% and 2% (*w/v*) HES as previously mentioned. Dynamic shear moduli of each NaHA solution were measured by small amplitude oscillatory shear experiments over the frequency range of 0.1–2 Hz with a rotational rheometer (HAAKE Viscotester iQ Air, Thermo Fisher Scientific, Waltham, MA, USA) equipped with a Peltier temperature control module kept at 37 °C. The software HAAKE RheoWin (ver. 4.86, Thermo Fisher Scientific, Waltham, MA, USA) was used to determine storage ( $G'$ ) and loss ( $G''$ ) shear moduli of NaHA solution at each frequency. Cone geometry with a diameter of 6 cm and core angle of 2° was used. Prior to frequency sweep experiments, strain amplitude was confirmed by strain sweep experiments to be sufficiently small to provide a linear material response at all investigated frequencies. A solvent trap was used to avoid evaporation of samples during experiments. Experiments were carried out at least eight times.

Dynamic shear moduli of NaHA solutions with and without HES were measured immediately before shear stress loading at the rate of 0.1 s<sup>-1</sup> and every 2 h from shear stress loading up to 8 h. The relaxation time of the NaHA solution according to the Maxwell model [21] was also calculated before and at the end of shear stress loading (i.e., 0 h and 8 h, respectively).

### 2.4. Convective Transport of FHA

FHA was dissolved in 0.15 M NaCl solution to prepare 0.1% (*w/w*) solution as previously mentioned for NaHA. Experiments for convective transport of FHA were carried out using the ultra-fast, double-sided reusable sample dialyzer<sup>TM</sup> as described above. In this system, 0.5 mL of FHA solution was interposed between two pre-cut polyvinylidene Durapore<sup>®</sup> membrane filters (0.1 µm in pore size, cut to fit 24 mm diameter; VVLP025000, Merck Millipore, Burlington, MA, USA). Then, 0.15 M NaCl solution or 0.5%, 1%, or 2% HES solution was infused via a tube attached to the system at a rate of 20 µL/min for 6 h using an automatic infusion pump as mentioned above. The fluid flow rate in the sample dialyzer<sup>TM</sup> was calculated to be 1.9 µm/s. The system was placed in an incubator (IC101W, Yamato Scientific, Tokyo, Japan) kept at 37 °C. The fluid outflow from the dialyzer<sup>TM</sup> was drained into the UV flow cell (72/Q/10, capacity 1.8 mL; Starna Scientific, Essex, UK) via a connecting tube, and the absorbance of FHA in the UV flow cell was measured at 444 nm (absorption wavelength) every 0.2 min for 6 h using a UV spectrometer (Model UV-1850; Shimadzu, Kyoto, Japan). The temperature of the UV flow cell was maintained at 37 °C with a temperature control unit (Model TCC-100; Shimadzu, Kyoto, Japan). Experiments were carried out five times.

Quantities of FHA contained in the beam passage space of the UV flow cell at time =  $t$  ( $Q(t)$ , g) were determined from the UV absorbance of FHA at time =  $t$  ( $Abs(t)$ ) by comparing the absorbance of FHA with a calibration line of the relationship between fluorescence intensity and known concentrations of FHA:

$$Q(t) = \frac{V_s}{\epsilon} \cdot Abs(t), \quad (5)$$

where  $V_s$  is the volume of the beam passage space of the UV flow cell (i.e., 0.24 mL) and  $\epsilon$  is the absorption coefficient (mL/g). Total quantities of FHA outflow from the UV flow cell during the experiments were also obtained and expressed as values relative to FHA quantity in the dialyzer<sup>TM</sup> before fluid infusion.

### 2.5. Statistical Analysis

Values were compared among NaHA solutions with or without HES by one-way analysis of variance and by two-way repeated measures analysis of variance, with solvent (NaCl or HES solution) as the factor and time points as repeated factors using SigmaPlot 13 (Systat Software Inc., Chicago, IL, USA) software. Statistical significance was reported according to several values of the  $p$  criterion (i.e.,  $p < 0.05$ ;  $p < 0.01$ ;  $p < 0.001$ ). Values are expressed as mean  $\pm$  standard deviation.

## 3. Results and Discussion

### 3.1. Effects of HES on Hydraulic Conductivity ( $K$ ) of NaHA Solution

In the presence of 1% HES, the  $\kappa$  values of NaHA solution at 0.1–0.5% decreased by 30–70% compared to 0.15 M NaCl solution alone (Figure 2a). This is consistent with previous result that 2% HES decreased Darcy's permeability coefficients of 0.1–0.5% NaHA [18]. This finding may be explained by the friction between NaHA and HES arising from hydrogen bond formation due to polysaccharidal nature of these molecules, as suggested by the decrease in the flow activation energy of NaHA by HES [17].

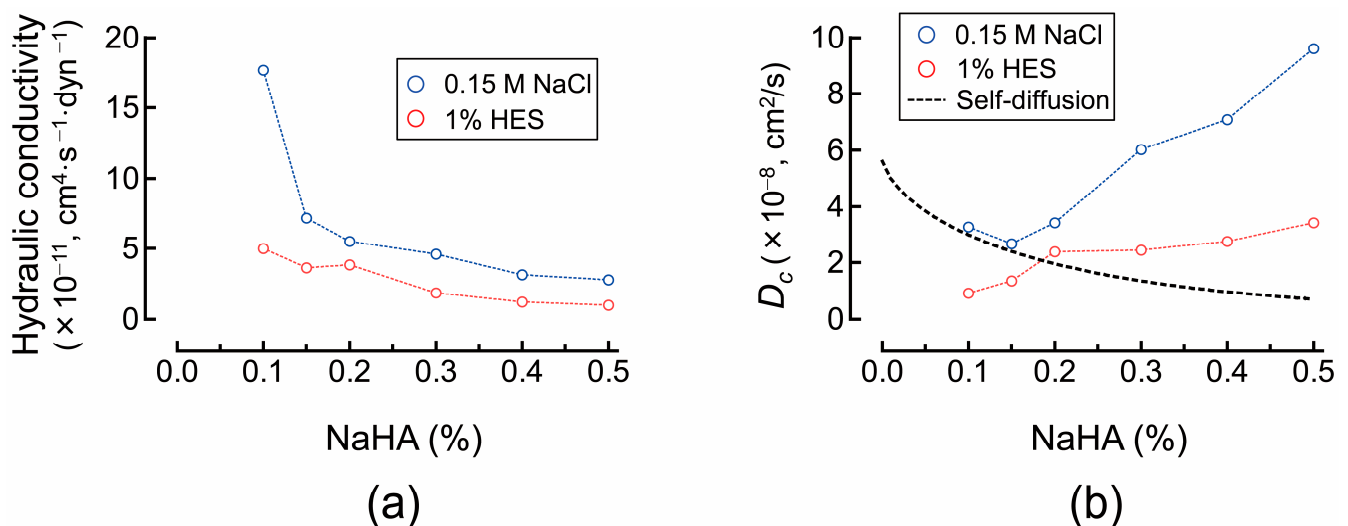


**Figure 2.** (a) Hydraulic conductivity of sodium hyaluronic acid (NaHA) in 0.15 M NaCl solution or 1% hydroxyethyl starch (HES) solution. Experiments were carried out at 25 °C. (b) Collective diffusion coefficient ( $D_c$ ) of sodium hyaluronic acid (NaHA) in 0.15 M NaCl solution or 1% hydroxyethyl starch (HES) solution. The dashed line denotes data for the self-diffusion coefficient of hyaluronic acid ( $M_w: 0.83 \times 10^6$ ) in phosphate-buffered saline (pH 7.4) at 25 °C from the literature [16].

The  $D_c$  of NaHA in 0.15 M NaCl solution alone, which was the lowest at 0.15% NaHA, increased with increasing NaHA concentration. The  $D_c$  of NaHA solution alone was similar to the self-diffusion constant previously reported in the literature [16] at concentrations lower than 0.15%. The addition of 1% HES decreased the  $D_c$  of NaHA of 0.1–0.5% to 30–70% of that of 0.15 M NaCl solution alone (Figure 2b). This suggests that HES locally restricts NaHA dispersion, which explains the decrease in the intrinsic viscosity of NaHA by HES [17].

### 3.2. Effects of HES on Dynamic Shear Moduli of NaHA Solution during Shear Stress Loading

The addition of HES to NaHA solution did not significantly change the  $G'$  of the NaHA solution. On the other hand, the addition of HES significantly increased the  $G''$  of the NaHA solution before shear stress loading at all frequencies compared to the  $G''$  of NaHA in 0.15 M NaCl solution alone (e.g.,  $p < 0.001$  at 0.36 Hz, Figure 3).



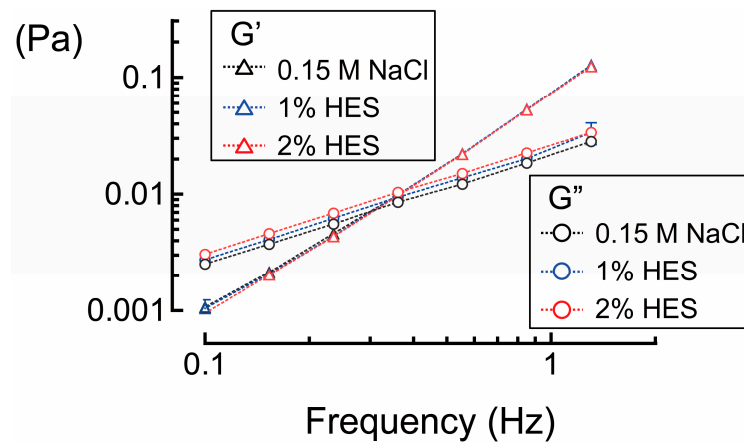


**Figure 3.** Storage ( $G'$ ) and loss ( $G''$ ) shear moduli of 0.1% sodium hyaluronic acid dissolved in 0.15 M NaCl solution, 1% hydroxyethyl starch (HES) solution, or 2% HES solution before shear loading. Experiments were carried out at 37 °C. Values are expressed as mean and standard deviation ( $n = 11$  (NaCl) or 8 (HES)).

While the  $G'$  of NaHA in 0.15 M NaCl solution alone did not significantly change over time during shear stress loading, the  $G''$  of NaHA in 0.15 M NaCl solution alone decreased during shear stress loading compared to before shear stress loading (e.g., by 22% at 4 h and by 29% at 8 h at 0.36 Hz) (Figure 4a).

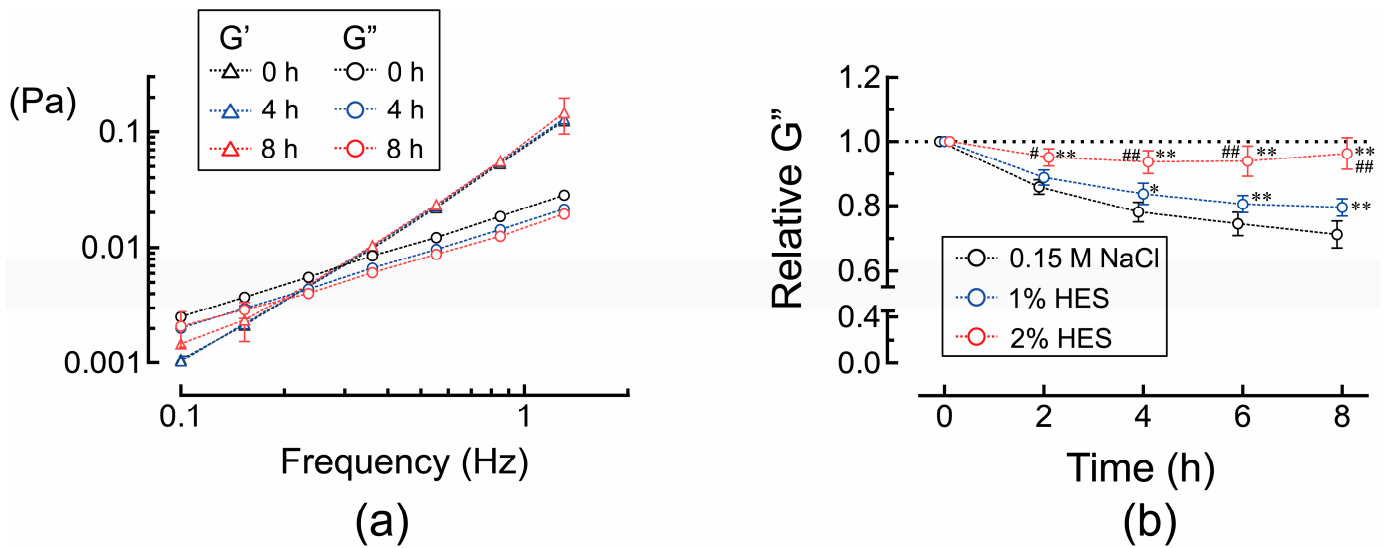


**Figure 4.** (a) Storage ( $G'$ ) and loss ( $G''$ ) shear moduli of 0.1% sodium hyaluronic acid (NaHA) dissolved in 0.15 M NaCl solution before shear stress loading (0 h), at 4 h after the start of shear stress loading, and at the end of shear stress loading (8 h). Experiments were carried out at 37 °C. Values are expressed as mean and standard deviation ( $n = 11$  (NaCl) or 8 (HES)). (b) Time-course changes in loss shear moduli ( $G''$ ) of 0.1% sodium hyaluronic acid dissolved in 0.15 M NaCl solution, 1% hydroxyethyl starch (HES) solution, or 2% HES solution at 0.36 Hz during shear stress loading relative to before shear stress loading. Values are expressed as mean and standard deviation. There were significant differences among time points except 6 h vs. 8 h ( $p < 0.001$ ). \*:  $p < 0.01$  versus 0.15 M NaCl; \*\*:  $p < 0.001$  versus 0.15 M NaCl; #:  $p < 0.01$  versus 1% HES; ###:  $p < 0.001$  versus 1% HES.

The presence of HES in the NaHA solution significantly attenuated the decrease in the  $G''$  of NaHA solution during shear stress loading at 0.36 Hz ( $p < 0.001$ , Figure 4b); the  $G''$  of NaHA solution at 8 h relative to 0 h was  $0.71 \pm 0.04$  in 0.15 M NaCl alone,  $0.80 \pm 0.03$  with 1% HES, and  $0.96 \pm 0.05$  with 2% HES. These changes in  $G''$  before and after shear stress loading were found to be irreversible.

The relaxation time of NaHA was significantly shorter in the presence of HES than 0.15 M NaCl solution alone at 0 h and 8 h (Table 1). Shear stress loading increased the relaxation time by 60% in 0.15 M NaCl solution alone ( $p < 0.001$ ), and the presence of 2% HES did not significantly change the relaxation time after shear stress loading.

**Table 1.** Relaxation time (s) of 0.1% sodium hyaluronic acid in 0.15 M NaCl solution alone or hydroxyethyl starch (HES) solution before (0 h) and at the end (8 h) of shear stress loading.

Solvent	0 h	8 h	<i>p</i> Value <sup>1</sup>
0.15 M NaCl	0.53 ± 0.04	0.82 ± 0.10	<0.001
1% HES	0.44 ± 0.02 *	0.63 ± 0.03 **	<0.001
2% HES	0.41 ± 0.02 **, #	0.44 ± 0.03 **, ##	0.22

Values are presented as mean and standard deviation ( $n = 11$  (NaCl) or 8 (HES)). <sup>1</sup> 0 h versus 8 h. \*:  $p < 0.05$  versus 0.15 M NaCl; \*\*:  $p < 0.001$  versus 0.15 M NaCl; #:  $p < 0.05$  versus 1% HES; ##:  $p < 0.001$  versus 1% HES.

Given that shear stress loading decreased the  $G''$ , but not  $G'$ , of NaHA in NaCl solution alone over time (Figure 4a), it is unlikely that shear loading caused the degradation of NaHA, as a decrease in the molecular weight of HA is expected to decrease both  $G'$  and  $G''$  [22]. Since  $G''$  refers to the viscous modulus, representing the amount of energy dissipated as heat [21], the finding suggests a decrease over time in friction between NaHA and the solvent (i.e., NaCl or HES solution) during shear stress loading. The friction between NaHA and HES, as reflected by the decrease in the  $D_c$  of NaHA in the presence of HES (Figure 2b), explains why the decrease in the  $G''$  of NaHA during shear stress loading was attenuated by the addition of HES. This is supported by the fact that no significant increase in relaxation time was observed before and after shear stress loading in the presence of 2% HES (Table 1). As shear stress can cause disorientation of NaHA, the findings in this study suggest that HES may preserve the structure of NaHA by inhibiting NaHA disorientation under fluid shear stress, probably due to a stiffening of NaHA structure via hydrogen bonds between NaHA and HES [17].

### 3.3. Effects of HES on Convective Transport of FHA

After the complete passage of FHA through the dead space of the connecting tube, the relative quantity of FHA in the UV flow cell showed a transient peak at approximately 2 h (Figure 5a). HES solutions showed significantly higher peaks of relative FHA quantities ( $0.30 \pm 0.03$  with 0.5% HES;  $0.25 \pm 0.02$  with 1% HES;  $0.26 \pm 0.03$  with 2% HES) compared to NaCl solution alone ( $0.11 \pm 0.01$ ) ( $p < 0.001$ ). The infusion of 0.5% HES solution significantly increased the total relative quantity of FHA outflow from the UV flow cell ( $0.94 \pm 0.05$ ) compared to the NaCl solution alone ( $0.42 \pm 0.04$ ) ( $p < 0.001$ ) (Figure 5b).

The HES-induced acceleration of convective transport of FHA may be attributed to the increase in the dragging of NaHA by HES due to the friction between NaHA and HES. This mechanism may be relevant to previous findings that HES decreased the intrinsic viscosity of NaHA [17] and thereby accelerated the diffusion of small molecules through NaHA solution [18].

Another explanation is the decrease in the  $D_c$  of NaHA by HES. Solute flux ( $J_s$ ) is described in terms of a combination of diffusion and convection, as follows [23]:

$$J_s = -K_d D_\infty \nabla C + K_c v C \quad (6)$$

where  $C$  is the solute concentration,  $v$  is the fluid velocity,  $K_d$  is the diffusive hindrance factor (the diffusivity of the fluid divided by the diffusivity of free solution  $D_\infty$ ), and  $K_c$  is the convective hindrance factor (the solute-to-fluid velocity ratio under conditions where diffusion is negligible and the solute behaves as a freely suspended particle). Accordingly, the quantity of FHA outflow from the dialyzer<sup>TM</sup> is determined by the balance between the  $K_d$  and  $K_c$  of FHA. As the FHA quantity in the UV flow cell started to increase at similar times with or without HES (i.e., around 2 h, Figure 5a), it is unlikely that HES

changed the  $K_c$  of FHA. Instead, according to the simulation (Figure 6a), the decrease in  $D_c$  is expected to increase the peak height of solute quantity in the UV flow cell (Figure 6b). This computational result supports the scenario that HES increased the peak heights of FHA quantities in the UV flow cell by decreasing the  $D_c$  (i.e.,  $K_d D_\infty$ ) of FHA.

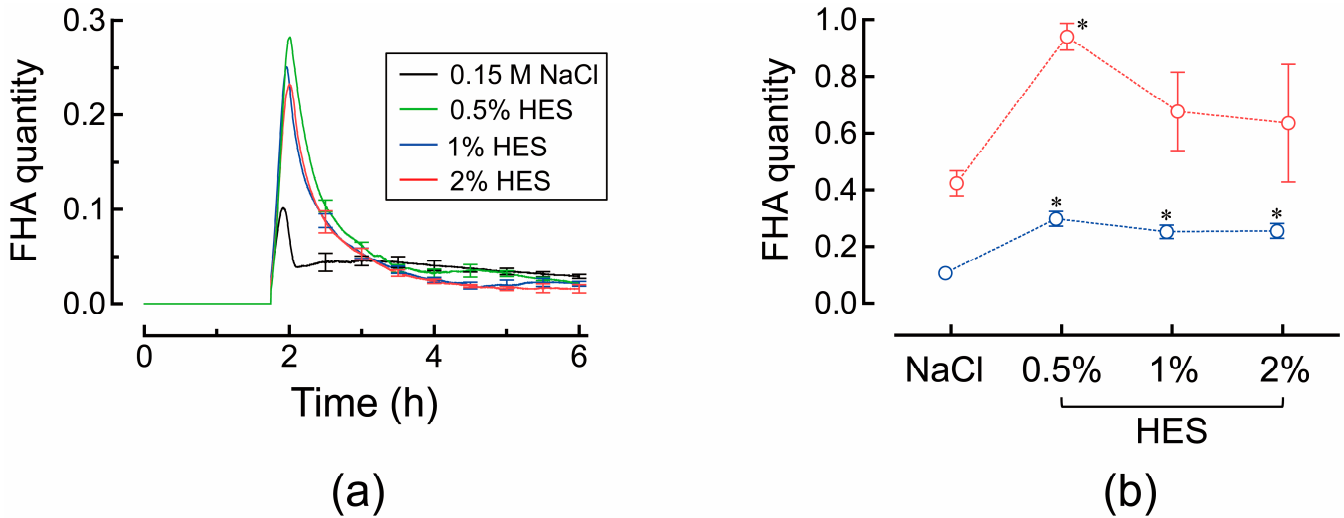


**Figure 5.** (a) Time-course quantities of fluorescein-labeled hyaluronic acid (FHA) in the UV flow cell during fluid (0.15 M NaCl solution or 0.5%, 1%, or 2% hydroxyethyl starch (HES) solution) flow relative to that in the dialyzer™ before fluid flow. Experiments were carried out at 37 °C. Values after 2.5 h are expressed as mean and standard deviation ( $n = 5$ ) every 0.5 h. (b) Comparison of peak quantities of fluorescein-labeled hyaluronic acid (FHA) in the UV flow cell (blue circle) and total quantities of FHA outflow from the UV flow cell (red circle) during fluid (0.15 M NaCl solution or 0.5%, 1%, or 2% hydroxyethyl starch (HES)) flow relative to FHA quantities in the dialyzer™ before fluid flow. Values are expressed as mean and standard deviation. \*:  $p < 0.001$  versus NaCl.

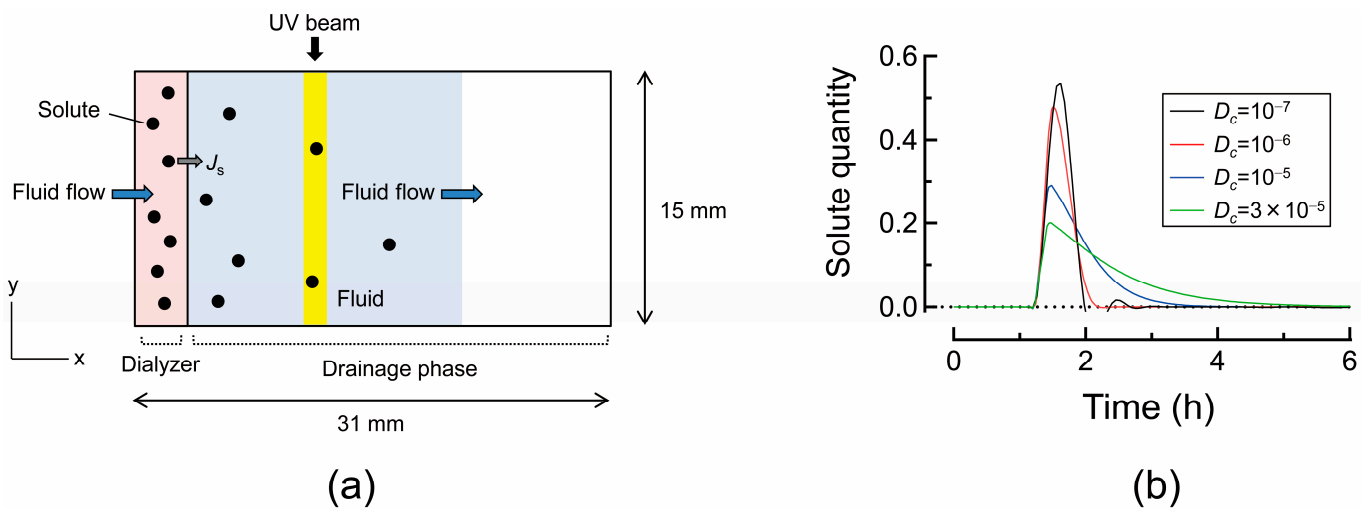


**Figure 6.** (a) A schematic for the simulation of convective transport of solute. A two-dimensional finite element model with fluid flow in the horizontal direction at a rate of  $1.9 \mu\text{m/s}$  was formulated with natural boundary conditions. Finite element analysis for time-course changes of solute quantity in the slit of the UV flow cell relative to solute quantity in the dialyzer™ before fluid flow was performed with the commercially available finite element software FlexPDE (version 7.2, PDE Solutions Inc., Spokane, WA, USA). For simplicity of simulation, the y-direction lengths of the dialyzer™ and drainage phase were assumed to be the same.  $J_s$ : solute flux. (b) Computational results from the finite element model with fluid flow in the horizontal direction. Solute quantity in



the vertical axis denotes the solute quantity in the slit of the UV flow cell relative to that in the dialyzer™ before fluid infusion.  $D_c$ : diffusion coefficient of solute in  $\text{cm}^2/\text{s}$ . Convective hindrance factor of solute was assumed to be 1.

### 3.4. Implications

The findings of this study have clinical relevance, especially in cancer patients receiving HES infusion during major surgery. Cancer tissue is characterized by a high interstitial fluid pressure and high interstitial fluid flow rate due to its large hydraulic conductivity, resulting in the accelerated interstitial diffusion and convection of solutes [8,24]. The concentration range of HES used in this study (0.5–1%) corresponds to concentrations of HES assumed to be present in the interstitium of inflammatory tissue in clinical settings. In order to identify the effects of HES on NaHA, the present study tested a low concentration of NaHA (i.e., 0.1%) in normal interstitium [1,2], because higher NaHA concentrations enhance the intermolecular interaction between NaHA chains [3]. High concentrations of HA may result in different changes in NaHA's rheological properties during shear stress, as demonstrated in the preliminary study showing that the shear-induced distortion of NaHA (i.e.,  $G''$  decrease) was less pronounced for 0.3% NaHA solution compared to that for 0.1% NaHA solution (Figure S2 in Supplementary File).

Given that the shear-induced distortion of HA allows the easier mobilization of HA in the interstitium, HES-induced attenuation of shear distortion of HA is expected to preserve HA distribution in the interstitium and thus low hydraulic conductivity of the interstitium. This is beneficial for the prevention of tumor cell metastasis because increased interstitial fluid flow accelerates tumor cell migration into lymphatic vessels [11]. On the contrary, when collagen is degraded by collagenase under inflammatory conditions [25], HA is easily mobilized from the interstitium into lymphatic vessels due to accelerated convection by HES. The resulting loss of HA in the interstitium allows for easier transport of therapeutics into tumor cells (Figure 7).

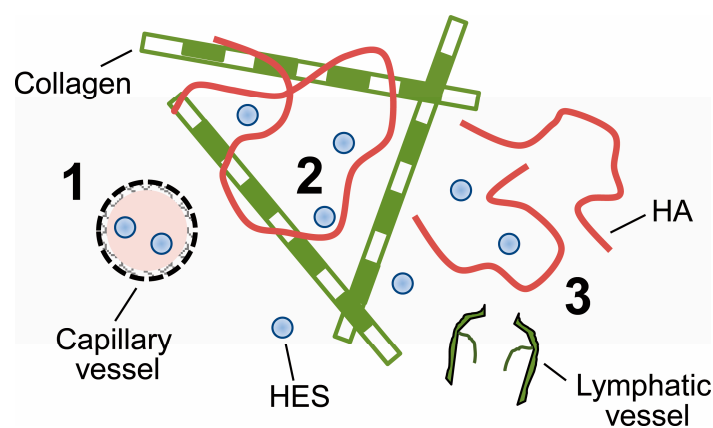


**Figure 7.** Key roles of hydroxyethyl starch (HES) in the intercellular space: (1) restore blood volume, (2) attenuate shear-induced deformation of hyaluronic acid (HA), (3) accelerate the convective transport of HA.

### 4. Conclusions

This study measured the hydraulic conductivity of NaHA solution and the dynamic viscoelasticities of NaHA during shear stress loading and convective transport of FHA with or without HES for the purpose of investigating the effects of HES on HA's structure and distribution under flow conditions. HES decreased the hydraulic conductivity of the NaHA solution, leading to the slowed collective diffusion of NaHA. HES also attenuated the shear-induced distortion of NaHA, but accelerated the convective transport of FHA.

Given the important roles of HA in pathologies such as inflammation and cancer, the HES-induced modification of HA structure and distribution in the interstitium should

be taken into account in the treatment of cancer patients undergoing major surgery. As this study has a limitation that the interactions of HA with coarse fixed elements such as collagen and other glycosaminoglycans such as chondroitin sulphate and heparan sulphate were not considered in terms of HA's rheological properties, these scenarios warrant further investigation in in vivo studies.

**Supplementary Materials:** The following supporting information can be downloaded at: <https://www.mdpi.com/article/10.3390/polysaccharides5040038/s1>, Figure S1: Osmotic pressure measurement of sodium hyaluronic acid solution; Figure S2: Time-course changes in loss shear moduli of sodium hyaluronic acid of different concentrations during shear stress loading.

**Funding:** This work was funded by Grants-in-Aid for Scientific Research JSPS KAKENHI (Grant number 22K09033).

**Institutional Review Board Statement:** Not applicable.

**Data Availability Statement:** The original contributions presented in the study are included in the article; further inquiries can be directed to the corresponding author.

**Conflicts of Interest:** The author declares no conflicts to declare.

## References

1. Levick, J.R. Flow through interstitium and other fibrous matrices. *Q. J. Exp. Physiol.* **1987**, *72*, 409–437. [[CrossRef](#)] [[PubMed](#)]
2. Comper, W.D.; Laurent, T.C. Physiological function of connective tissue polysaccharides. *Physiol. Rev.* **1978**, *58*, 255–315. [[CrossRef](#)] [[PubMed](#)]
3. Cowman, M.K.; Matsuoka, S. Experimental approaches to hyaluronan structure. *Carbohydr. Res.* **2005**, *340*, 791–809. [[CrossRef](#)] [[PubMed](#)]
4. Fouissac, E.; Milas, M.; Rinaudo, M. Shear-rate, concentration, molecular weight, and temperature viscosity dependences of hyaluronate, a wormlike polyelectrolyte. *Macromolecules* **1993**, *26*, 6945–6951. [[CrossRef](#)]
5. Laurent, T.C. In vitro studies on the transport of macromolecules through the connective tissue. *Fed. Proc.* **1966**, *25*, 1128–1134. [[PubMed](#)]
6. Laurent, T.C. Structure of the extracellular matrix and the biology of hyaluronan. In *Interstitial, Connective Tissue and Lymphatics*; Reed, R.K., McHale, N.G., Bert, J.L., Winlove, C.P., Laine, G.A., Eds.; Portland Press: London, UK, 1995; pp. 1–12.
7. Levick, J.R. *An Introduction to Cardiovascular Physiology*, 5th ed.; Hodder Education: London, UK, 2010; pp. 188–219.
8. Wiig, H.; Swartz, M.A. Interstitial fluid and lymph formation and transport: Physiological regulation and roles in inflammation and cancer. *Physiol. Rev.* **2012**, *92*, 1005–1060. [[CrossRef](#)] [[PubMed](#)]
9. Cowman, M.K.; Lee, H.-G.; Schwertfeger, K.L.; McCarthy, J.B.; Turley, E.A. The content and size of hyaluronan in biological fluids and tissues. *Front. Immunol.* **2015**, *6*, 261. [[CrossRef](#)] [[PubMed](#)]
10. Swartz, M.A.; Fleury, M.E. Interstitial flow and its effects in soft tissues. *Annu. Rev. Biomed. Eng.* **2007**, *9*, 229–256. [[CrossRef](#)] [[PubMed](#)]
11. Swartz, M.A.; Lund, A.W. Lymphatic and interstitial flow in the tumour microenvironment: Linking mechanobiology with immunity. *Nat. Rev. Cancer* **2012**, *12*, 210–219. [[CrossRef](#)] [[PubMed](#)]
12. Westphal, M.; James, M.F.M.; Kozek-Langenecker, S.; Stocker, R.; Guidet, B.; Van Aken, H. Hydroxyethyl starches: Different products—Different effects. *Anesthesiology* **2009**, *111*, 187–202. [[CrossRef](#)] [[PubMed](#)]
13. Woodcock, T.E.; Woodcock, T.M. Revised Starling equation and the glycocalyx model of transvascular fluid exchange: An improved paradigm for prescribing intravenous fluid therapy. *Br. J. Anaesth.* **2012**, *108*, 384–394. [[CrossRef](#)] [[PubMed](#)]
14. Fujii, K.; Kawata, M.; Kobayashi, Y.; Okamoto, A.; Nishinari, K. Effects of the addition of hyaluronate segments with different chain lengths on the viscoelasticity of hyaluronic acid solutions. *Biopolymers* **1996**, *38*, 583–591. [[CrossRef](#)]
15. Kurata, M.; Tsunashima, Y. Viscosity—Molecular weight relationships and unperturbed dimensions of linear chain molecules. In *Polymer Handbook*, 4th ed.; Brandrup, J., Immergut, E.H., Grulke, E.A., Eds.; John Wiley & Sons, Inc.: New York, NY, USA, 1999; pp. VII/1–VII/83.
16. Gribbon, P.; Heng, B.C.; Hardingham, T.E. The molecular basis of the solution properties of hyaluronan investigated by confocal fluorescence recovery after photobleaching. *Biophys. J.* **1999**, *77*, 2210–2216. [[CrossRef](#)] [[PubMed](#)]
17. Tatara, T. Contrasting effects of albumin and hydroxyethyl starch solutions on physical properties of sodium hyaluronate solution. *Carbohydr. Polym.* **2018**, *201*, 60–64. [[CrossRef](#)] [[PubMed](#)]
18. Tatara, T. Different effects of albumin and hydroxyethyl starch on low molecular-weight solute permeation through sodium hyaluronic acid solution. *Polymers* **2021**, *13*, 514. [[CrossRef](#)] [[PubMed](#)]
19. Doi, M. *Soft Matter Physics*; Oxford University Press: Oxford, UK, 2018; pp. 137–164.
20. Laurent, T.C.; Ogston, A.G. The interaction between polysaccharides and other macromolecules. 4. The osmotic pressure of mixtures of serum albumin and hyaluronic acid. *Biochem. J.* **1963**, *89*, 249–253. [[CrossRef](#)] [[PubMed](#)]

21. Rubinstein, M.; Colby, R.H. *Polymer Physics*; Oxford University Press: Oxford, UK, 2018; pp. 253–305.
22. Snetkov, P.; Zakharova, K.; Morozkina, S.; Olekhovich, R.; Uspenskaya, M. Hyaluronic acid: The influence of molecular weight on structural, physical, physico-chemical, and degradable properties of biopolymer. *Polymers* **2020**, *12*, 1800. [[CrossRef](#)] [[PubMed](#)]
23. Kosto, K.B.; Deen, W.M. Hindered convection of macromolecules in hydrogels. *Biophys. J.* **2005**, *88*, 277–286. [[CrossRef](#)] [[PubMed](#)]
24. Jain, R.K. Transport of molecules in the tumor interstitium: A review. *Cancer Res.* **1987**, *47*, 3039–3051. [[PubMed](#)]
25. Chen, W.Y.; Abatangelo, G. Functions of hyaluronan in wound repair. *Wound Repair Regen.* **1999**, *7*, 79–89. [[CrossRef](#)] [[PubMed](#)]

**Disclaimer/Publisher’s Note:** The statements, opinions and data contained in all publications are solely those of the individual author(s) and contributor(s) and not of MDPI and/or the editor(s). MDPI and/or the editor(s) disclaim responsibility for any injury to people or property resulting from any ideas, methods, instructions or products referred to in the content.